Available online at www.sciencedirect.com

ScienceDirect

Procedia IUTAM 15 (2015) 2 – 13

Procedia IUTAM

www.elsevier.com/locate/procedia

IUTAM Symposium on Multiphase flows with phase change: challenges and opportunities, Hyderabad, India (December 08 – December 11, 2014)

Direct numerical simulations of flows with phase change

Grétar Tryggvason[a], Jiacai Lu[a]

[a]*University of Notre Dame, Notre Dame, IN 46556, USA*

Abstract

Direct Numerical Simulations (DNS) of multiphase flows, where every continuum length and time scale are fully resolved, currently allow us to simulate flows of considerable complexity, such as the motion of several hundred bubbles or drops in turbulent flows, for sufficiently long time so that meaningful statistical quantities can be obtained. Additional physical processes such as heat transfer and phase change have also been included, although only for relatively small systems so far. After reviewing briefly recent studies of bubbles in turbulent channel flows, we discuss simulations of flows with phase change, focusing on bubble generation by boiling. The addition of new physics often results in new length and time scales that are shorter and faster than the dominant flow scales. Similarly, very small features such as thin films, filaments, and drops can also arise during coalescence and breakup of fluid blobs. The geometry of these features is usually simple, since surface tension effects are strong and inertia effects are relatively small and in isolation these features are often well described by analytical or semi-analytical models. Recent efforts to embed analytical and semi-analytical models to capture such features, in combination with direct numerical simulations of the rest of the flow, are discussed. We conclude by a short discussion of the use of DNS data for closure laws for model equations for the large scale flow.

Peer-review under responsibility of Indian Institute of Technology, Hyderabad.

Keywords:

1. Introduction

Computational studies of multiphase flows started at the beginning of computational fluid dynamics, when the MAC method of Harlow and collaborators was used for simulations of the Rayleigh-Taylor instability, splashes due to impacting droplets, and other problems involving a free surface or a fluid interface [1,2,3]. Although some of the results produced by the MAC method and early versions of the VOF method [4] are impressive, particularly in light of the primitive computational resources available in the sixties and early seventies, widespread interest in such simulations did not take off until the beginning of the nineties, when significant improvements in methods that use fixed grids (as used in the MAC and the VOF method) took place. Progress included the continuous surface force (CSF) approach [5]

* Corresponding author. Tel.: +0-000-000-0000 ; fax: +0-000-000-0000.
E-mail address: gtryggva@nd.edu

Peer-review under responsibility of Indian Institute of Technology, Hyderabad.
doi:10.1016/j.piutam.2015.04.002

to compute surface tension in VOF methods, the level set[6], phase field[7] and CIP[8] methods, and the front tracking method of Unverdi & Tryggvason[9]. By now a large number of refinement and new methods have been introduced and the development of numerical methods for multiphase flow has been a "hot" topic for some time. The development of more efficient, accurate, and robust methods continues to be of considerable interest, but it is the use of these methods to increase our understanding of complex flows, as well as the extension of the methods to handle more complex physics, where the most exciting action is. Direct numerical simulations (DNS) where all continuum temporal and spatial scales are accurately resolved for systems of sufficient size so that non-trivial scale interactions take place are, in particular, proving to yield major new insight, even though DNS have only been used to examine a tiny fraction of the systems that can be explored with current capabilities. The overwhelming majority of those studies have been concerned with disperse multiphase flows, where one phase is continuous and the other one appears as bubbles or drops. While a number of multiphase flows have been examined by DNS, bubbly flows have perhaps received most attention. Here we first review briefly recent studies of bubbly flows and then discuss simulations of the formation of bubbles by boiling.

2. DNS of Bubbly Flows

Several investigators have examined the motion of single bubbles, but our interest has been in understanding the dynamics of systems with large number of bubbles. For early DNS of bubbles in fully periodic domains, see Unverdi and Tryggvason[9], Esmaeeli and Tryggvason[10,11,12], Bunner and Tryggvason[13,14,15], for example. Later studies have focused on flows in channels[16,17 18,19,20]. For nearly spherical buoyant bubbles in vertical channels we have found that the insight provided by the DNS results allowed us to essentially solve the problem analytically. For upflow and downflow, independently of whether the flow is laminar or initially turbulent, the middle region is in hydrostatic balance where the weight of the mixture is such that it balances exactly the imposed pressure gradient. This observation allows us to write down a very simple analytical expression for what the void fraction in the center should be, given the imposed pressure gradient and the average void fraction. For upflow, the void fraction in the core is lower than the average, and knowing that we can predict how many bubbles move to the wall. For downflow the void fraction must increase and the number of bubbles that must be taken from the wall region determines its thickness, which again, is given by a simple, formula. For downflow the velocity in the wall region is given either by a parabolic velocity profile in the laminar case or by the law of the wall for the turbulent case. Since the velocity in the center is controlled by what happens in the wall layer, the total flow rate is thus easily predicted. For upflow the velocity in the wall layer is not as easily predicted due to the presence of bubbles, but the simplicity of the layer suggests several possible approximations. As the bubbles became deformable they no longer drift to the wall but stay in the middle of the channel. The flow rate is reduced significantly when the bubbles drift to the wall, but this reduction is not seen for the deformable bubbles. Most recently we have done a series of simulations where only the deformability of the bubbles is changed (by changing surface tension)[21] and this study shows that the flow is relatively insensitive to the exact value of the surface tension as long as the bubbles remain nearly spherical and there was a well-defined bubble-rich wall-layer. As the deformability increased, the flow abruptly transitions to a very different state where the bubbles do not accumulate near the walls, but remain in the middle of the channel. In this new state the main effect of the bubbles is to make the mixture lighter than single-phase liquid and once the pressure gradient is adjusted to account for the weight of the mixture, the flow structure is remarkably similar to what is seen for single-phase flow. Changing the deformability of the bubbles in this new state has little effect on the liquid flow rate and other characteristics of the flow, as long as the bubbles do not break up. Although considerable information was available for these flows experimentally, the DNS study provided both additional information and helped us bring it all together in ways not possible before.

Our examination of the statistically steady state flows of bubbles in laminar and turbulent flows in vertical channels have already lead to considerable insight into relatively simple flows where the bubbles are all of the same size. These results should eventually lead to improved models that can be used to make industrial scale prediction of multiphase flows. We have[22] compared flow in laminar channels with average model[23] and found that upflow was very sensitive to the tunable parameters of the model but for downflow the model predictions were very robust. we have also[24] examined the transient motion of a cluster of bubbles across a horizontal channel and showed that the void fraction evolution is accurately described by a simple drift-flux-like model.

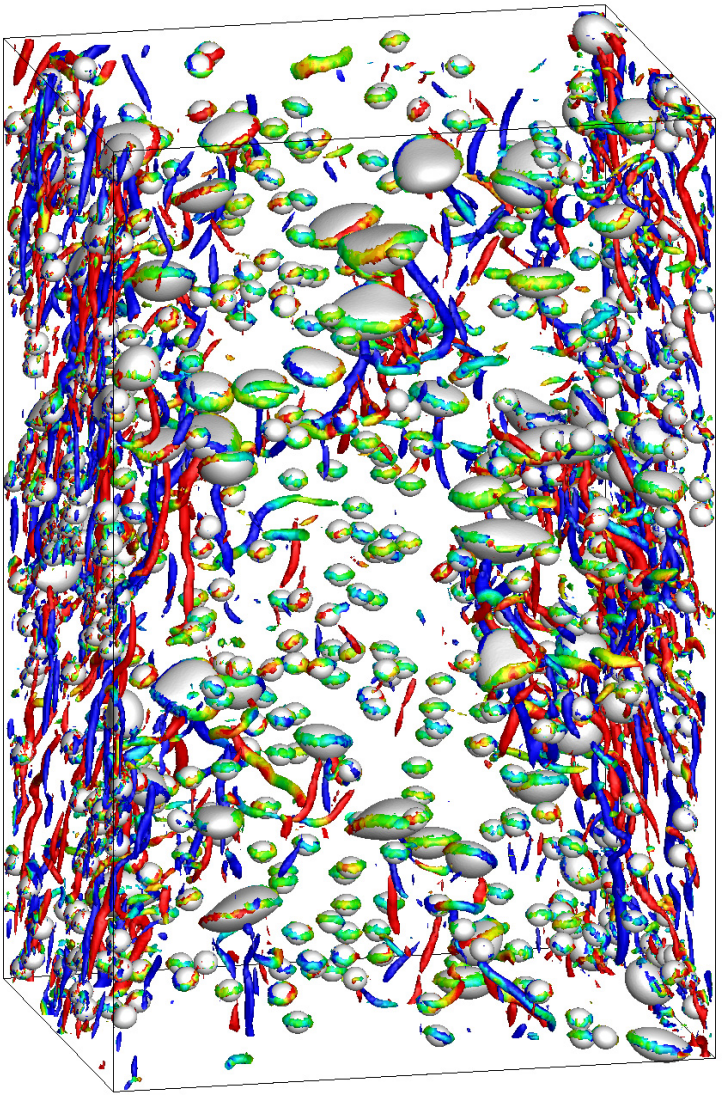

Fig. 1. One frame from a large simulation of many bubbles of different sizes rising upward in turbulent channel flow. The bubbles and vortical structures identified by the λ_2 method[25] are shown. Preliminary results were also shown in Tryggvason et al.[26].

So far, we have mostly focused on the long time results where the flow has reached an approximately statistically steady state. This simplifies the data analysis since it allows us to average over time (in addition to space) and also allows comparisons with the hydrostatic model. The transient evolution is, however, important for several reasons. First of all, it is relatively long so in practical applications it is likely that it is encountered frequently and possibly more often than the steady state, and secondly, the relatively simple structure of the flow at steady state is not very sensitive to the various parameters in models of the average flow evaluation. The void fraction distribution does, for example, only depend on the sign of the bubble lift coefficient but not its magnitude. To understand how bubbly flow evolves toward a steady state we have conducted several simulations, starting with bubbles placed randomly in a parabolic laminar velocity field. The results show that when nearly spherical bubbles are injected into parabolic flow, the evolution toward steady state is highly non-monotonic. First all the bubbles migrate towards the walls, leaving the center region nearly free of bubbles. Then the presence of the bubbles near the wall increases the shear there and

reduces the flow rate. As the flow rate is reduced some of the bubbles migrate back into the core region until the mixture there is in hydrostatic equilibrium. The initial migration of the bubbles to the wall takes place relatively fast, but the slowing down of the flow and the migration of the bubbles back into the core is much slower.

To examine what happens for turbulent flows with bubbles of different sizes, we are currently doing simulations with several hundred bubbles injected into turbulent flow. The domain size is $2\pi \times 4 \times \pi$ computational units in the streamwise, wall-normal and spanwise direction, respectively, resolved by 0.4 Billion grid points. The physical parameters are selected such that the Morton number is equal to 5.75×10^{-10} and the void fraction is 0.0304. The bubbles come in four sizes, with the smallest bubbles having a diameter of 0.16 in computational units, and the largest one with a diameter of 0.44. The majority of the bubbles are small and we expect the smallest two sets of bubbles to accumulate at the wall. The numbers of bubbles for each group were selected so that there are enough small bubbles that can be pushed to the wall to put the core into hydrostatic equilibrium. The properties of the fluid and the bubbles are the same as in our earlier simulations, but the domain size is eight times larger, giving a friction Reynolds number of $Re^+ = 500$. The bubbles are initially distributed nearly uniformly across the domain but as they start to rise, the smaller bubbles start to migrate toward the walls and form a dense wall-layer. In figure 1 we show the bubbles at a relatively early time, where many of the small bubbles have moved to the wall, but the there are still several small bubbles in the middle, along with most of the larger bubbles. The bubbles are shown along with the vorticity, visualized using the λ_2 method[25]. To understand the vortical structure a little better, we color the vortical structures according to their orientation. Thus, both red and blue vortical structures are aligned with the flow, but red have a positive rotation while the blue ones have a negative rotation. The intermediate colors (light blue, green and yellow) indicate vortical structures that are not aligned with the flow. As expected, the majority of the vortical structures aligned with the flow come in pairs, such that a blue structure is frequently found next to a red one. The figure shows that the longitudinal vortices that one expects in turbulent boundary layers do appear to survive the addition of the bubbles to the wall-layer, at least at the time plotted here, and suggests that vorticity shed by the large bubbles is responsible for the majority of the vorticity in the interior of the channel. Vortices that are mostly horizontal do, for the most part, encircle bubbles.

As important as bubbly flows are, they usually represent only one aspect of a real engineering problem. In most cases we have to deal with something else simultaneously, such as the transfer of mass or heat. Extension of numerical methods to such flows are starting to appear[27,26] and in the next section we discuss bubble formation by boiling.

3. DNS of Boiling

In essentially all DNS of dispersed bubbly flows it has been assumed that the bubbles already exist at the start of the simulations. Yet, in reality the bubbles must be injected into the flow or be generated in some other way. Often this is by boiling. We have extended the method of Unverdi and Tryggvason[9] to boiling flows[28,29] and used it to examine a number of problems. Those include explosive boiling of a nucleus in an initially superheated liquid[29] and film boiling on a flat plate[30,31]. For the film boiling we examined, in particular, how large systems, where bubbles broke off from the vapor film at the wall, differed from systems where the bubble growth was forced to take place at the linearly most-unstable wavelength. The main question was whether subharmonic instabilities would lead to competition between waves and the formation of larger bubbles. Such mergers are seen in many other systems, but here we found that such competition was relatively weak. We also examined the effect of the wall superheat on the boiling of a finite depth pool. For low wall superheat (but high enough to prevent wetting and a transition to nucleate boiling) bubbles broke away from the vapor film. At higher superheat the vapor production was sufficiently fast so that long vapor vents formed, sometimes reaching the surface of the pool. At even higher superheat the vents became unsteady, resulting in unsteady churn-like boiling. For moderate superheat where the vapor dynamics was much faster than the total evaporation rate of the pool, the system reached a well-defined steady state, but at high superheat all the liquid quickly evaporated and no steady state emerged.

More recently we have been focusing on nucleate boiling where bubbles are generated from nucleation sites on a wall and below we first review the equations governing boiling and then show a couple of examples of simulations of bubbles originating at walls. In addition to considerable difficulties (mostly unsolved so far) associated with specifying the nucleation site distribution and activation, we do, in principle, need to account for the thin microlayer left behind when the vapor bubble expands. In the examples shown here the micro layer is not included.

The transport of heat is governed by the energy equation and for simulations of boiling, it must be solved in addition to the momentum and mass conservation equations. Here we will assume that except for the volume change at the phase boundary, the flow is incompressible and that heat generation due to internal friction can be neglected. The energy equation, simplified somewhat, is therefore

$$\frac{\partial}{\partial t}(\rho cT) + \nabla \cdot \rho cT\mathbf{u} = \nabla \cdot k\nabla T + \dot{q}\delta(n), \tag{1}$$

where $\delta(n)$ is a one dimensional delta function of the normal coordinate n. Integrating the energy equation across the phase boundary gives the source term

$$\dot{q} = k\frac{\partial T}{\partial n}\bigg)_l - k\frac{\partial T}{\partial n}\bigg)_g. \tag{2}$$

Since the interface temperature can be taken to be equal to the saturation temperature, a term involving the differences in the specific heats is zero. In addition to the energy equation, an interface condition on the temperature must be satisfied at the phase boundary. For a large number of situations of interest it is reasonable to assume a temperature equilibrium such that the temperature is continuous across the phase boundary and $T_l = T_g = T_f$, where, T_l and T_g are the temperatures in the liquid and the vapor at the interface, respectively, and T_f is the interface temperature. The temperature of the phase boundary can be found by careful consideration of the thermodynamics at the boundary and for a detailed derivation see, for example, Alexiades and Solomon [32]. For boiling we are usually justified in simply taking the temperature at the phase boundary to be equal to the saturation temperature of the liquid $T_f = T_v(P_{sys})$, where P_{sys} is the system pressure and can be assumed to be constant [28].

Since we assume that both the liquid and the vapor are incompressible and the only change of density is due to the phase change at the phase boundary, the momentum equation written for the entire flow field is

$$\frac{\partial(\rho\mathbf{u})}{\partial t} + \nabla \cdot (\rho\mathbf{u}\mathbf{u}) = -\nabla p - \rho\mathbf{g} + \nabla \cdot \mu\Big(\nabla\mathbf{u} + \nabla\mathbf{u}^T\Big) + \sigma\kappa\mathbf{n}\delta(n). \tag{3}$$

Integrating it across the phase boundary, assuming that it is infinitely thin, yields the jump conditions $[[-\rho\mathbf{u}\mathbf{u} - P\mathbf{n} + \mu(\nabla\mathbf{u} + \nabla\mathbf{u}^T)]] = \sigma\kappa\mathbf{n}$. The brackets denote the difference between the vapor and the liquid side. The first term, the difference in the momentum fluxes across the interface, is zero if there is no phase change and results from the acceleration of the fluid as liquid is converted into vapor. For a flat interface, where viscous stresses and surface tension can be neglected, this term must be balanced by a jump in the pressure across the interface.

At the phase boundary there is volume expansion. Writing $\mathbf{u} = \mathbf{u}_g H + \mathbf{u}_l(1-H)$, where the velocity in each phase is assumed to have a smooth incompressible extension into the other phase and using that the $\nabla \cdot \mathbf{u}_g = \nabla \cdot \mathbf{u}_l = 0$, yields:

$$\nabla \cdot \mathbf{u} = (u_g - u_l)\delta(n). \tag{4}$$

Here, the normal velocity of the liquid next to the boundary is u_l and the velocity of the vapor is u_g. The normal component of the velocity of the phase boundary is V_n and since there is a change of phase at the phase boundary, u_l, u_g and V_n are all unequal. If the liquid is evaporating, V_n is smaller than u_l and since the density of the vapor is much lower than the liquid, u_g is much larger than u_l. The rate of evaporation of liquid is equal to the difference in the velocity of the phase boundary and the liquid velocity, times the density of the liquid $\rho_l(u_l - V_n)$. Similarly, the rate of production of vapor is equal to the difference in the velocity of the phase boundary and the vapor velocity, times the density of the vapor, $\rho_g(u_g - V_n)$. Since mass is conserved, these two are equal, and the mass transfer rate at the phase boundary is:

$$\dot{m} = \rho_l(u_l - V_n) = \rho_g(u_g - V_n). \tag{5}$$

The volume expansion per unit interface area is found by eliminating V_n:

$$u_g - u_l = \dot{m}\Big(\frac{1}{\rho_g} - \frac{1}{\rho_l}\Big). \tag{6}$$

The normal velocity of the phase boundary can be written as:

$$V_n = \frac{1}{2}(u_l + u_g) - \frac{\dot{m}}{2}\Big(\frac{1}{\rho_l} + \frac{1}{\rho_g}\Big). \tag{7}$$

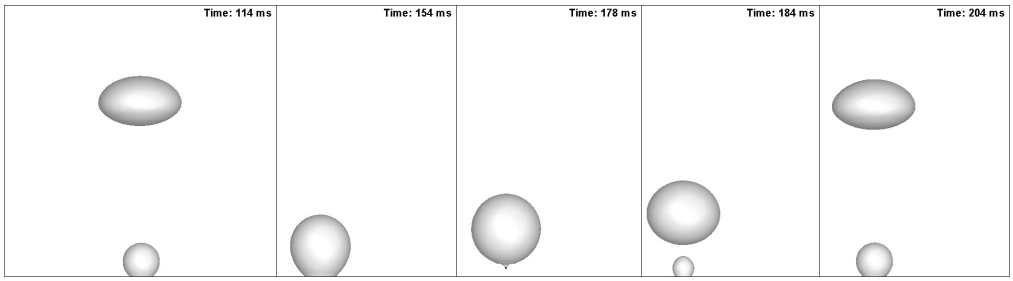

Fig. 2. Growth of a vapor bubble from a single nucleation site. The wall temperature is constant and the simulation is run for four full bubble generation cycles.

The rate of heat release at the phase boundary is the rate of evaporation multiplied by the latent heat h_{lg}, or $\dot{q} = h_{lg}\dot{m}$. so we can write

$$\nabla \cdot \mathbf{u} = \frac{\dot{q}}{L}\Big(\frac{1}{\rho_g} - \frac{1}{\rho_l}\Big)\delta(n). \tag{8}$$

The expression for the velocity of the phase boundary and the evaporation rate can also be found directly using the Rankine-Hugenoit conditions, derived by writing the mass conservation equation in a frame of reference moving with the phase boundary and integrating across the boundary[33].

Once the relative velocity of the phase boundary has been found, its position can be evolved in time by integrating

$$\frac{\mathbf{x}_f}{dt} = (\mathbf{u} + V_f\mathbf{n}), \tag{9}$$

where $\mathbf{u}$ is the average fluid velocity, at the phase boundary.

Thus, the computations of flow with phase change progress in more or less the same way as computations of non-evaporating flow. The major differences are that the pressure equation (derived from equation 8) includes a volume source term and the boundary conditions must be modified to allow the fluid to expand or contract; and the computation of the heat source at the interface, using equation (2). To compute the gradient of the temperature for the heat source we use the "normal probe" technique[34]. In this approach we draw a line segment normal to the interface and interpolate the temperature at the end of the segment (usually about one and a half grid spacing or so away from the interface). This temperature, along with the given interface temperature is then used to find the temperature gradient and the heat source.

The computational method introduced by Dhir and collaborators[35] follows more or less the strategy outlined above, except the interface is tracked using a level set method and vapor is assumed to be at the saturation pressure. The source term is therefore simplified. Several authors[36,37] have taken a different approach where they allow the interface temperature to deviate from the saturation temperature and then taker the mass flux to be proportional to the temperature difference. The theoretical foundation for this is not entirely clear, but this can perhaps be taken to be the zeroth iteration of the scheme used by Juric and Tryggvason[28]. In any case, this seems to work reasonably well.

The equations for boiling also apply to solidification, with the addition that the velocity in the solid is usually zero, but unlike boiling it is sometimes possible to ignore the change in volume[38,39]. In other cases the volume change is important[40].

While simulations of phase change away from solid boundaries are reasonably well under control, nucleate boiling is of much more practical interest. Such simulations have been done by a number of researchers[35,41,42] but their weakness remains the resolution of the thin layer of liquid left on the wall as the bubble expands. The evaporation of this layer is believed to contribute significantly to the growth of the vapor bubble. In figure 2 we show one example of the growth of a vapor bubble in water, from a single nucleation site in an initially quiescent pool. The wall temperature T_{wall} is kept constant at $110^{\circ}C$, the saturation temperature is $T_{sat} = 100^{\circ}$ C, and the initial water temperature is set as the saturation temperature. The computation domain size is $7.5\ mm \times 7.5\ mm \times 7.5\ mm$, and resolved by $64 \times 64 \times 64$ grid points. The initial bubble diameter is 0.8 mm and the contact angle is 45°. The bubble is shown at five times,

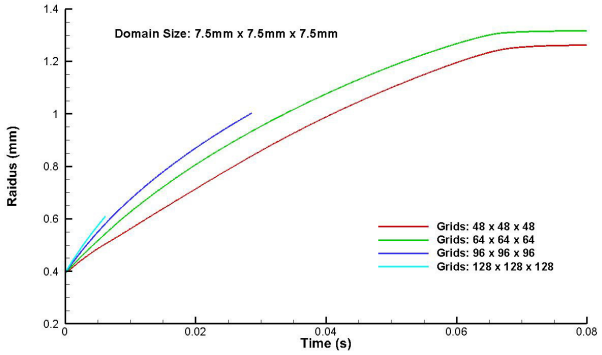

Fig. 3. The effective radius of a vapor bubble growing from a single nucleation site for different resolutions.

after the bubble formation has been repeated a few times. In the first frame a vapor bubble has just left the site and another one is in the process of being formed. In the third frame this bubble breaks off the site and another bubble starts to grow. The first bubble departs after 86 ms, with a departure diameter of 2.6 mm. The third and forth bubble are essentially the same and depart after 84 ms with departure diameter of 2.6 mm. The effect of resolution is shown in figure 3 where we plot the bubble radius versus time for several resolutions. Although the simulation on the finest grid has not progressed as far in time as the rest, it is clear that as the grid is refined, the results are converging. In those simulations no micro layer model is included and comparisons with experiments show that while the size of the bubble when it departs is in reasonably good agreement with experimental predictions, the bubble growth rate is much faster in the experiment. This is expected to be due to the evaporation of the micro-layer.

Another example from a simulation of nucleate boiling is shown in figures 4, 5 and 6 where we simulate the growth and release of a single bubble from a vertical wall, again leaving out the micro layer. In figure 4 (where we have tilted the frame so gravity points to the left and the bubbles rise to the right) the vapor bubble is shown at a few times, both for liquid flowing upward (top) and quiescent liquid (bottom). The governing parameter are different than in the previous example and selected to make it possible to use a relatively coarse grid. Thus, we take the ratio of the density, viscosity and conductivity to be only ten, corresponding to boiling at high pressure. For the bubble released into a flowing fluid, the initial velocity increases linearly with the distance from the wall. The initial evolution is similar in both cases but then the vapor bubble in the quiescent liquid departs from the wall, while the one in flow hugs the wall, while moving faster upward. The temperature field, at three times, is shown in figure 5 for both cases. The liquid is initially at saturation temperature but the hot wall has generated a hot liquid layer into which the bubble grows. As the bubbles move upward they disrupt this hot layer, pushing it outward ahead and drawing colder liquid toward the wall in their wake. The bubble distance from the wall and their volumes are shown in figure 6. Initially the bubbles stay close to the wall, but then the bubble growing into quiescent liquid lifts from the wall while the bubbles in flow stays close to the wall. The bubble is rising in a shear flow next to the wall and rising with a velocity that exceeds that of the liquid. This results in a lift force that will keep it close to the wall, until it has grown so big that the lift force changes sign or becomes zero. The volume of both bubbles increases at a comparable rate, even though the one in the flow rises faster, until the bubble in quiescent flow departs from the wall and its growth slows down.

4. Multiscale Models for Small Scales

The goal of DNS of multiphase flows is generally to use the results to elucidate how the large-scale structure of the flow depends on the interactions of the bubbles or drops with each other and the flow, as in the simulation shown in figure 1. Thus, it is generally important to examine as large systems as possible, to incorporate non-trivial scale interactions. The range of scales that can be covered is set by the resolution requirement. For a given number of grid points, the number required to resolve the smallest structures obviously determines how many structures can be included. Frequently there is a well-defined “dominant” scale, such as the size of the bubbles or drops, that is determined by the balance of surface tension and viscosity or inertia and where the appropriately chosen non-

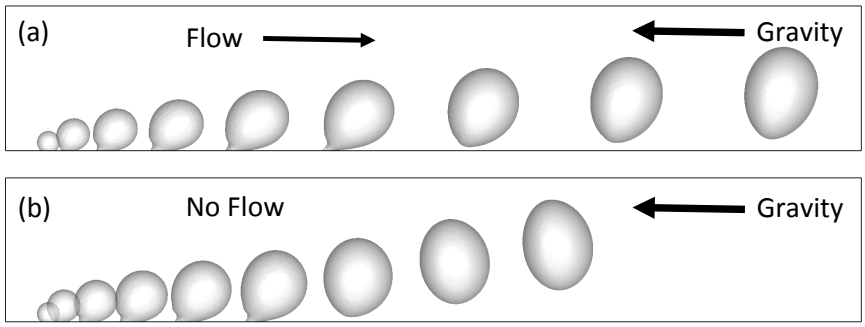

Fig. 4. The generation of vapor bubbles by nucleate boiling from a vertical wall. The bubble is shown at several times as it grows and rises along the wall due to buoyancy. In the top frame the liquid velocity increases linearly with distance from the wall.

dimensional numbers are of the order of unity. Sometimes, however, we encounter much smaller scales. These are often the results of interactions of elementary structures, such as the thin film between colliding bubbles or drops and—if the interaction results in topology changes—thin threads and tiny drops. Small scales can also emerge due to additional physics that evolves on different time and spatial scales than the flow of the "dominant" structures. Many authors have used various adaptive grid refinement strategies to resolve these small-scale features. However, such strategy generally consumes significant fraction of the available grid resolution and carries considerable overhead. Two things are generally true about the small-scale features: First of all, surface tension effects are strong and that keeps the geometry simple and, secondly, viscous effects are strong so the flow is simple. These are exactly the characteristics that invite an analytical treatment and a rather obvious strategy is therefore to resolve the small-scale motion using embedded analytical (or semi-analytical) descriptions that are coupled to a conventional numerical treatment of the rest of the flow. We have used this approach to capture small-scale processes for a few problems. In Thomas, Esmaeeli and Tryggvason[43], we used embedded analytical descriptions to capture the thin film between a sloping wall and a drop falling on it, and the subsequent sliding of the drop down the wall. Most of the flow was well resolved, but not the thin film between the drop and the sloping wall and for it a thin film model was used. Outside the film we applied the usual no-slip boundary conditions when computing the flow field, but where the film was, the wall-shear stress, as found from the film model, was prescribed. Although the film model that we used was very simple, it allowed us to simulate the motion relatively accurately on a grid where the film was not fully resolved. Comparison with results from calculations done on a very fine grid, where the film was resolved, showed good agreement and significant differences with results from calculations where the analytical description was not used. Although this simulation was for a relatively simple problem, where the location of the film was easily identified, the general approach should also work for more complex problems such as collisions of freely moving drops. This is also the approach taken for the modeling of the micro layer for nucleate boiling, although relatively poor understanding of the physics has proven to be an impediment to fully successful models.

The need for a multi scale approach can also come from additional physics, such as for mass transfer from bubbles, where the large discrepancy in the diffusivity of mass and momentum leads to very thin mass boundary layers. The physics is rather simple. Mass diffuses from the bubble surface and is then swept by the flow toward the back where it is carried away as the flow separates. The Schmidt number is defined as the ratio of viscosity and mass diffusivity ($Sc = \nu/D$), where ν is the kinematic viscosity and D is the mass diffusivity) and for high Schmidt numbers, the mass boundary layer is thin and can be difficult to resolve numerically. To derive a description to capture the mass transfer in a boundary layer that is so thin that it is not resolved, we decompose the scalar field into two fields, one resolved on the grid and the other captured by a boundary layer description. Since the advection-diffusion equation is linear, in principle these two fields can evolve independently. Where the boundary layer remains thin, the boundary layer accounts for all the mass that diffuses out from the bubble and the mass field resolved on the grid does not "know" about it. There is, in particular, no flux of mass from the bubble to the grid-mass field. For those parts of the bubble surface where the boundary layer is thick, we transfer the mass from the boundary layer and follow it using advection resolved on the grid. We note that while mass diffuses from the bubble into the boundary layer along its

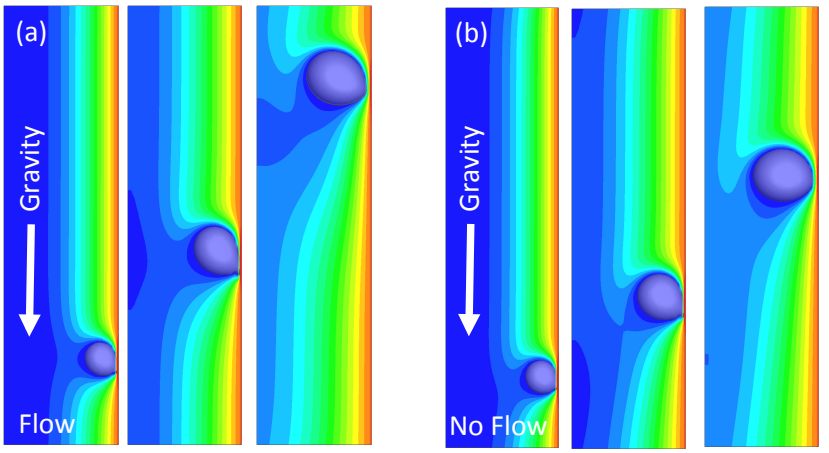

Fig. 5. The temperature field around the bubbles in figure 4 at three times. In the frames on the left the fluid is flowing upward but on the right there is no flow.

entire length, mass only leaves the boundary layer where it is "thick." In general, we can have several thick segments of the boundary layer along the bubble surface and this results in several coupling points. The basic formulation of this approach, along with results for two-dimensional flows, is described in Aboulhasanzadeh et al.[44], where we tested the accuracy of the model by comparing results using the boundary layer with calculations where the mass transfer was fully resolved. Generally the agreement is very good. We have also compared the results of a three-dimensional implementation with experimental results, specially designed to test our method, and with experimental correlations from the literature, and in both cases we find excellent agreement[45]. The new method has also been used to examine in some detail the effect that bubble-bubble interactions have on the mass transfer of freely moving bubbles[46].

Thin films have been coupled with computations of the rest of the flow by other investigators[47,48,41,49]. Another example of the use of an embedded analytical description can be found in Takagi et al.[50], where analytical solutions to the Stokes equation are used to describe the flow next to the surface of a solid particle. Furthermore, the point particle model for dilute flow of very small particles is yet another example of the use of an analytical solution for small-scale processes in fully resolved computation of the rest of the flow (the point particle model is often used for larger particles, but this is an approximation). While several authors have explored the use of embedded analytical descriptions for multiphase flow simulations, this is still a fairly experimental approach that needs to be tested for each new application. It is, however, very powerful when it works and as our experience with this approach to multi scale modeling increases, it is likely that it will be possible to put it on a firmer theoretical foundation that allows us to determine when it will work and when it does not, along with guidelines about how to ensure that the error is within some prescribed bounds.

5. Conclusion

We conclude by briefly mentioning yet another issue that is emerging as detailed DNS results for larger and larger multiphase systems have become available. It has become increasingly clear that the most critical challenge for these simulations to yield useful results is not that the simulations are not big enough but that the current multifluid and multiphase models are not sophisticated enough to make full use of the results. This is perhaps not surprising. With only a few exceptions, the current state-of-the-art in modeling the large-scale or average behavior of multiphase flows is the two-fluid model[51,52]. In studies of turbulent single-phase flows the availability of DNS data has lead to the development of a number of new models for the large-scale flow that have in turn motivated new simulations. With a few exceptions, attempts to use DNS results to help modeling efforts are still rare. Perhaps the most intense effort has been by a group mostly located in Grenoble, who has published several papers on LES modeling of multiphase flows where the filtered LES equations are derived, the unresolved terms identified and results of an *a priori* test

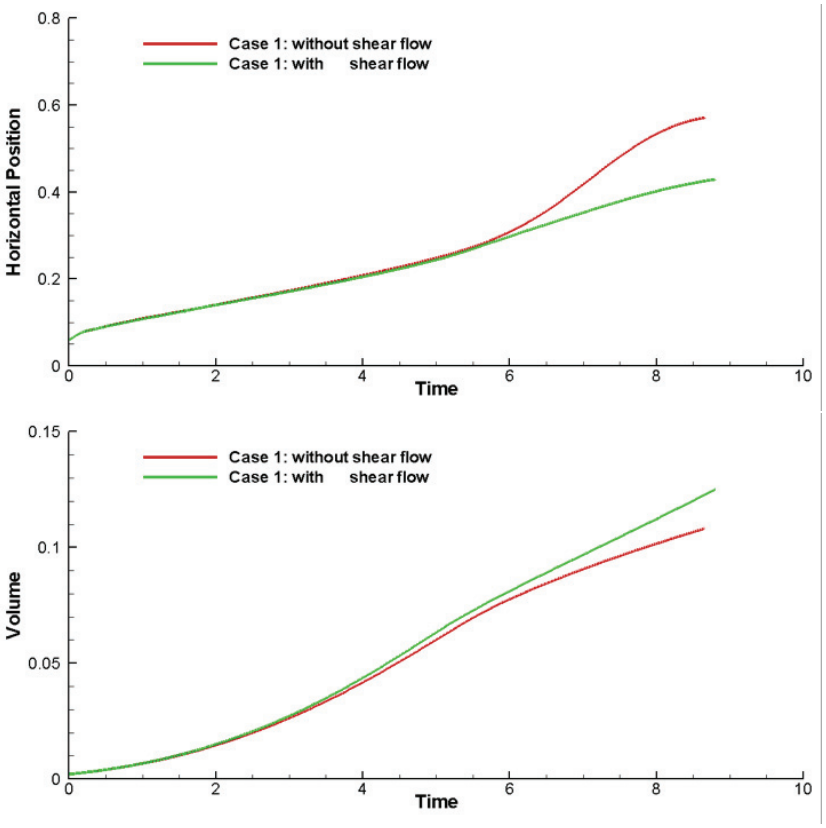

Fig. 6. The distance of the centroid of the vapor bubbles in figure 4 from the wall versus time (top frame) and the volume of the bubbles versus time (bottom frame).

are shown[53,54,55,56]. It is likely that further developments of the ideas presented in these papers, along with new approaches, will be one of the more exciting development in the applications of DNS to multiphase flows in the near future.

Acknowledgements

This study was supported by the Consortium for Advanced Simulation of Light Water Reactors (CASL). This research used resources of the Oak Ridge Leadership Computing Facility at the Oak Ridge National Laboratory, which is supported by the Office of Science of the U.S. Department of Energy under Contract No. DE-AC05-00OR22725.

References

1. Harlow, F.H., Welch, J.E.. Numerical calculation of time-dependent viscous incompressible flow of fluid with a free surface. *Phys Fluid* 1965;**8**:2182–2189.
2. Harlow, F.H., Welch, J.E.. Numerical study of large-amplitude free-surface motions. *Phys Fluid* 1966;**9**:842–851.
3. Harlow, F.H., Shannon, J.P.. The splash of a liquid drop. *J Appl Phys* 1967;**38**:3855–3866.
4. Hirt, C.W., Nichols, B.D.. Volume of Fluid (VOF) method for the dynamics of free boundaries. *J Comput Phys* 1981;**39**:201–226.
5. Brackbill, J.U., Kothe, D.B., Zemach, C.. A continuum method for modeling surface tension. *J Comput Phys* 1992;**100**:335–354.
6. Osher, S., Sethian, J.. Fronts propagating with curvature-dependent speed: algorithms based on Hamilton-Jacobi formulations. *J Comput Phys* 1988;**79**:12–49.
7. Jacqmin, D.. Calculation of two-phase Navier-Stokes flows using phase-field modeling. *J Comput Phys* 1999;**155**:96–127.

8. Takewaki, H., Yabe, T.. The cubic-interpolated pseudo particle (CIP) method: application to nonlinear and multi-dimensional hyperbolic equations. *J Comput Phys* 1987;**70**:355–372.
9. Unverdi, S.O., Tryggvason, G.. A front-tracking method for viscous, incompressible, multi-fluid flows. *J Comput Phys* 1992;**100**:25–37.
10. Esmaeeli, A., Tryggvason, G.. Direct numerical simulations of bubbly flows. Part I. Low Reynolds number arrays. *J Fluid Mech* 1998; **377**:313–345.
11. Esmaeeli, A., Tryggvason, G.. Direct numerical simulations of bubbly flows. Part II. Moderate Reynolds number arrays. *J Fluid Mech* 1999;**385**:325–358.
12. Esmaeeli, A., Tryggvason, G.. A direct numerical simulation study of the buoyant rise of bubbles at o (100) reynolds number. *Physics of Fluids* 2005;**17**:093303.
13. Bunner, B., Tryggvason, G.. Dynamics of homogeneous bubbly flows. Part 1. Rise velocity and microstructure of the bubbles. *J Fluid Mech* 2002;**466**:17–52.
14. Bunner, B., Tryggvason, G.. Dynamics of homogeneous bubbly flows. Part 2. Velocity fluctuations. *J Fluid Mech* 2002;**466**:53–84.
15. Bunner, B., Tryggvason, G.. Effect of bubble deformation on the stability and properties of bubbly flows. *J Fluid Mech* 2003;**495**:77–118.
16. Lu, J., Fernandez, A., Tryggvason, G.. The effect of bubbles on the wall shear in a turbulent channel flow. *Phys Fluids* 2005;**17**:095102.
17. Lu, J., Biswas, S., Tryggvason, G.. Laminar bubbly flow in a vertical channel. *Bulletin of the American Physical Society* 2005;.
18. Lu, J., Tryggvason, G.. Numerical study of turbulent bubbly downflows in a vertical channel. *Phys Fluids* 2006;**18**:103302.
19. Lu, J., Tryggvason, G.. Effect of bubble deformability in turbulent bubbly upflow in a vertical channel. *Phys Fluids* 2008;**20**:040701.
20. Lu, J., Tryggvason, G.. Dynamics of nearly spherical bubbles in a turbulent channel upflow. *Journal of Fluid Mechanics* 2013;**732**:166–189.
21. Dabiri, S., Lu, J., Tryggvason, G.. Transition between regimes of a vertical channel bubbly upflow due to bubble deformability. *Physics of Fluids* 2013;**25**.
22. Biswas, S., Esmaeeli, A., Tryggvason, G.. Comparison of results from dns of bubbly flows with a two-fluid model for two-dimensional laminar flows. *Int J Multiphase Flows* 2005;**31**:1036–1048.
23. Antal, S.P., Lahey, R.T., Flaherty, J.E.. Analysis of phase distribution in fully developed laminar bubbly two-phase flows. *Int J Multiphase Flow* 1991;**15**:635–652.
24. Biswas, S., Tryggvason, G.. The transient buoyancy driven motion of bubbles across a two-dimensional quiescent domain. *Int J Multiphase Flow* 2007;**33**.
25. Jeong, J., Hussain, F.. On the identification of a vortex. *J Fluid Mech* 1995;**285**:69–94.
26. Tryggvason, G., Thomas, S., Lu, J., Aboulhasanzadeh, B.. Multiscale issues in dns of multiphase flows. *Acta Mathematica Scientia* 2010; **30**(2):551–562.
27. Aboulhasanzadeh, B., Tryggvason, G.. A multiscale approach to compute mass transfer in bubbly flows. *Bulletin of the American Physical Society* 2011;**56**.
28. Juric, D., Tryggvason, G.. Computations of boiling flows. *Int J Multiphase Flow* 1998;**24**:387–410.
29. Esmaeeli, A., Tryggvason, G.. Computations of explosive boiling in microgravity. *J Scientific Computing* 2003;**19**:163–182.
30. Esmaeeli, A., Tryggvason, G.. Computations of film boiling. Part I: numerical method. *Int J Heat and Mass Transfer* 2004;**47**:5451–5461.
31. Esmaeeli, A., Tryggvason, G.. Computations of film boiling. Part II: multi-mode film boiling. *Int J Heat and Mass Transfer* 2004; **47**:5463–5476.
32. Alexiades, V., Solomon, A.D.. *Mathematical Modeling of Melting and Freezing Processes*. Hemisphere; 1993.
33. Esmaeeli, A., Tryggvason, G.. Computations of film boiling. part i: numerical method. *International journal of heat and mass transfer* 2004;**47**(25):5451–5461.
34. Udaykumar, H.S., Mittal, R., Shyy, W.. Computation of solid-liquid phase fronts in the sharp interface limit on fixed grids. *J Comput Phys* 1999;**153**:535–574.
35. Son, G., Dhir, V.K.. Numerical simulation of film boiling near critical pressures with a level set method. *J Heat Trans* 1998;**120**:183–192.
36. Hardt, S., Wondra, F.. Evaporation model for interfacial flows based on a continuum-field representation of the source terms. *Journal of Computational Physics* 2008;**227**:5871–5895.
37. Kunkelmann, C., Stephan, P.. Cfd simulation of boiling flows using the volume-of-fluid method within openfoam. *Numerical Heat Transfer, Part A: Applications* 2009;**56**:631–646.
38. Al-Rawahi, N., Tryggvason, G.. Numerical simulation of dendritic solidification with convection: two-dimensional geometry. *J Comput Phys* 2002;**180**:471–496.
39. Al-Rawahi, N., Tryggvason, G.. Numerical simulation of dendritic solidification with convection: Three-dimensional flow. *J Comput Phys* 2004;**194**:677–696.
40. Vu, T.V., Tryggvason, G., Homma, S., Wells, J.C., Takakura, H.. A front-tracking method for three-phase computations of solidification with volume change. *Journal of Chemical Engineering of Japan* 2013;**46**:726–731.
41. Son, G., Ramanujapu, N., Dhir, V.K.. Numerical simulation of bubble merger process on a single nucleation site during pool nucleate boiling. *ASME J Heat Transfer* 2002;**124**:51–62.
42. Son, G., Dhir, V.K.. Numerical simulation of nucleate boiling on a horizontal surface at high heat fluxes. *Int J Heat and Mass Transfer* 2008;**9-10**:2566–2582.
43. Thomas, S., Esmaeeli, A., Tryggvason, G.. Multiscale computations of thin films in multiphase flows. *International Journal of Multiphase Flow* 2010;**36**(1):71–77.
44. Aboulhasanzadeh, B., Thomas, S., Taeibi-Rahni, M., Tryggvason, G.. Multiscale computations of mass transfer from buoyant bubbles. *Chemical Engineering Science* 2012;**75**:456–467.
45. Aboulhasanzadeh, B., Hosoda, S., Tomiyama, A., Tryggvason, G.. A validation of an embedded analytical description approach to the computations of mass transfer from bubbles in high schmidt number liquids. *Chemical Engineering Science* 2013;**101**:165–174.
46. Aboulhasanzadeh, B., Tryggvason, G.. Effect of bubble interactions on mass transfer in bubbly flow. *International Journal of Heat and Mass Transfer* 2014;**79**:390–396.

47. Davis, R.H., Schonberg, J.A., Rallison, J.M.. The lubrication force between two viscous drops. *Physics of Fluids A: Fluid Dynamics* 1989; **1**:77–81.
48. Son, G., Dhir, V., Ramanujapu, N.. Dynamics and heat transfer associated with a single bubble during nucleate boiling on a horizontal surface. *J Heat Transfer* 1999;**121**:623–631.
49. Ge, Y., Fan, L.S.. Three-dimensional direct numerical simulation for film-boiling contact of moving particle and liquid droplet. *Phys Fluids* 2006;**18**:117104.
50. Takagi, S., Oguz, H.N., Zhang, Z., Prosperetti, A.. Physalis: A new method for particle simulation. part ii: Two-dimensional navier-stokes flow around cylinders. *Journal of Computational Physics* 2003;**187**:371–390.
51. Harlow, F.H., Amsden, A.A.. Numerical calculation of multiphase fluid flow. *Journal of Computational Physics* 1975;**17**:19–52.
52. Ishii, M.. *Thermo-Fluid Dynamic Theory of Two-Phase Flow*. Eyrolles; 1975.
53. E. Labourasse D. Lacanette, A.T., Lubin, P., Vincent, S., Lebaigue, O., Caltagirone, J.P., Sagaut, P.. Towards large eddy simulation of isothermal two-phase flows: Governing equations and a priori tests. *International Journal of Multiphase Flow* 2007;**33**:1–39.
54. Toutant, A., Labourasse, E., Lebaigue, O., Simonin, O.. Dns of the interaction between a deformable buoyant bubble and spatially decaying turbulence: a priori tests for les two-phase flow modelling. *Computers and Fluids* 2008;**37**:877–886.
55. Toutant, A., Chandesris, M., Jamet, D., Lebaigue, O.. Jump conditions for filtered quantities at an under-resolved interface. part 1: Theoretical developments. *International Journal of Multiphase Flow* 2009;**35**(1100-1118).
56. Toutant, A., Chandesris, M., Jamet, D., Lebaigue, O.. Jump conditions for filtered quantities at an under-resolved interface. part 2: A priori tests. *International Journal of Multiphase Flow* 2009;**35**:1119–1129.